Microalgae bio-reactive facade: a model coupling weather, illumination, temperature, and cell growth over the year Supplementary materials

Victor Pozzobon[1] ✉

[1]LGPM, CentraleSupélec, Université Paris-Saclay, Centre Européen de Biotechnologie et de Bioéconomie (CEBB), 3 rue des Rouges Terres 51110 Pomacle, France

Thermal model

The model is based on a heat balance between the biofaçade reservoir and its surrounding. It comprises:

- incident direct solar radiation (Φ_{Sun}, split into infrared radiation and visible light, Eq. 1). $\Phi_{Sun,Vis}$, being determined by the model proposed by the Illuminating Engineering Society (1), accounts for 48.7 % of total sun power (2), which allows to derive $\Phi_{Sun,IR}$ (Eq. 2),
- sky radiation (Eq. 3, 4, 5, and 6), calculated using a sky temperature model (3–5),
- surrounding radiation (Eq. 9, 10, 11, 12 and 13), accounting for Urban Heat Island effect (6–9),
- controlled absorption of the visible part of the radiative heat flux (Eq. 7) and associated reflectivities (Eq. 8) (10),
- indoor radiation (Eq. 14 and 15) (11),
- indoor convection using resistance in series modeling approach (Eq. 16, 17, and 18) (4, 11, 12),
- outdoor convection using resistance in series modeling approach (Eq. 19, 20, 21, and 22) and Defraeye's correlation to assess wind contribution (Table 1) (13, 14),
- power originated from the gas sparged into the reservoir (Eq. 23).

Combined together, they govern the temporal evolution of the biofaçade reservoir temperature (Eq. 24).

$$\Phi_{Sun} = \Phi_{Sun,Vis} + \Phi_{Sun,IR} \tag{1}$$

$$\Phi_{Sun,IR} = (\frac{1}{0.487} - 1)\Phi_{Sun,Vis} = 1.05\Phi_{Sun,Vis} \tag{2}$$

$$\Phi_{Sky,Tot} = \sigma\epsilon_{Sky}T^4_{Sky} \tag{3}$$

$$\begin{aligned}\epsilon_{Sky}T^4_{Sky} &= 9.36575\ 10^{-6}(1-CC)T^6_{Air,Out} \\ &+ T^4_{Air,Out}CC[(1-0.84CC)(0.527+0.161\ \exp(8.45[1-\frac{273}{T_{Air,Out}}]))+0.84CC]\end{aligned} \tag{4}$$

$$\Phi_{Sky,Abs} = F_{Sky}(0.4\ \tau_{Sun} + 0.6\ \tau_{Sky,Abs})(\frac{3-2\alpha^2-\alpha}{3}(1-\eta_{ps})\Phi_{Sky,Vis} + (\Phi_{Sky,Tot} - \Phi_{Sky,Vis})) \tag{5}$$

$$\Phi_{Sky,Emi} = F_{Sky}\tau_{Sky,Emi}\sigma\epsilon_{mc}T^4_{mc} \tag{6}$$

$$\Phi_{Sun,Abs} = \tau_{Sun}(\frac{3-2\alpha^2-\alpha}{3}(1-\eta_{ps})\Phi_{Sun,Vis} + 1.05\Phi_{Sun,Vis}) \tag{7}$$

$$R_{interface} = \frac{1}{2}\left[\frac{\tan^2(\theta_i-\theta_r)}{\tan^2(\theta_i+\theta_r)} + \frac{\sin^2(\theta_i-\theta_r)}{\sin^2(\theta_i+\theta_r)}\right] \tag{8}$$

$$UHII = \max(T_{Urb} - T_{Rur}) \tag{9}$$

$$UHII = -0.54\,\overline{U} - 1.48\,\overline{CC} - 0.039\,\overline{Y} + 7.63 \tag{10}$$

$$T_{Rur} = (1-CC)(2.82+1.15T_{Air,Out}) + CC(1.33+1.00T_{Air,Out}) \tag{11}$$

$$\Phi_{Sur,Abs} = F_{Sur}\tau_{Sur,Abs}\sigma\epsilon_{Sur}T_{Sur}^4 \tag{12}$$

$$\Phi_{Sur,Emi} = F_{Sur}\tau_{Sur,Emi}\sigma\epsilon_{mc}T_{mc}^4 \tag{13}$$

$$\Phi_{In,Rad,Abs} = \tau_{In,Rad,Abs}\sigma\epsilon_{In}T_{In}^4 \tag{14}$$

$$\Phi_{In,Rad,Emi} = \tau_{In,Rad,Emi}\sigma\epsilon_{mc}T_{mc}^4 \tag{15}$$

$$h_{In,Conv,Free} = 2.04\,(\frac{H_{mc}}{H_{Ref,In}}(T_{pmma,In} - T_{Air,In}))^{0.23} \tag{16}$$

$$h_{In,Conv,Forced} = \frac{k_{Air}}{L_{Ref}}\;0.664\;Re_{Ref}^{1/2}Pr^{1/3} = 0.72\text{ W/m²/K} \tag{17}$$

$$\Phi_{In,Conv,Net} = \frac{T_{Air,In} - T_{mc}}{\frac{1}{h_{In,Conv}} + \frac{e_{pmma}}{k_{pmma}}} \tag{18}$$

$$\overline{h_{Out,Conv,Free}} = \frac{k_{Air}}{E_{mc}}\left[0.825 + \frac{0.387\;Ra_L^{1/6}}{[1+(0.492\;Pr)^{9/16}]^{8/27}}\right]^2 \tag{19}$$

$$U_{Out} = U_{Station}\left(\frac{r_{Building}}{r_{Station}}\right)^{0.0706}\frac{\ln(\frac{E_{mc}+r_{Building}}{r_{Building}})}{\ln(\frac{E_{Station}+r_{Station}}{r_{Station}})} \tag{20}$$

$$h_{Out,Conv,Forced} = A_{\theta_{Wind}}U_{Out}^{B_{\theta_{Wind}}} \tag{21}$$

Wind incidence angle (θ_{Wind}, in degree)	$A_{\theta_{Wind}}$ ($W/m^2/K$)	$B_{\theta_{Wind}}$ (-)
0	4.90	0.86
30, 330	4.63	0.87
30, 300	4.25	0.88
90, 270	2.78	0.87
120, 240	1.44	0.83
150, 210	1.85	0.84
180	2.25	0.84

Table 1. Defraeye's correlation for different wind incidence angles on the facade. Couples of incidence angles tied to the same parameters originate from symmetry consideration

$$\Phi_{Out,Conv,Net} = \frac{T_{Air,Out} - T_{mc}}{\dfrac{1}{h_{Out,Conv}} + \dfrac{n_{Glaz} e_{pmma}}{k_{pmma}} + \dfrac{(n_{Glaz}-1) e_{Air}}{k_{Air}}} \tag{22}$$

$$P_{Gas,Net} = f H_{mc} w_{mc} e_{mc} \rho_{Gas} Cp_{Gas} (T_{Gas} - T_{mc}) \tag{23}$$

$$\begin{aligned} H_{mc} w_{mc} e_{mc} \rho_{Water} Cp_{Water} \frac{dT_{mc}}{dt} =& H_{mc} w_{mc} [\Phi_{Sun,Abs} + \Phi_{Sky,Abs} - \Phi_{Sky,Emi} + \Phi_{Sur,Abs} \\ & - \Phi_{Sur,Emi} + \Phi_{In,Rad,Abs} - \Phi_{In,Rad,Emi} + \Phi_{In,Conv,Net} \\ & + \Phi_{Out,Conv,Net}] + P_{Gas,Net} \end{aligned} \tag{24}$$

Performance distribution convergence analysis

Figure 1 reports the arithmetic mean and the standard deviation of the performance criteria as a function of the number of draws in the Sobol's sequence. As one can see, 2^8 draws are required to ensure a 2 % convergence on both the arithmetic mean and the standard deviation.

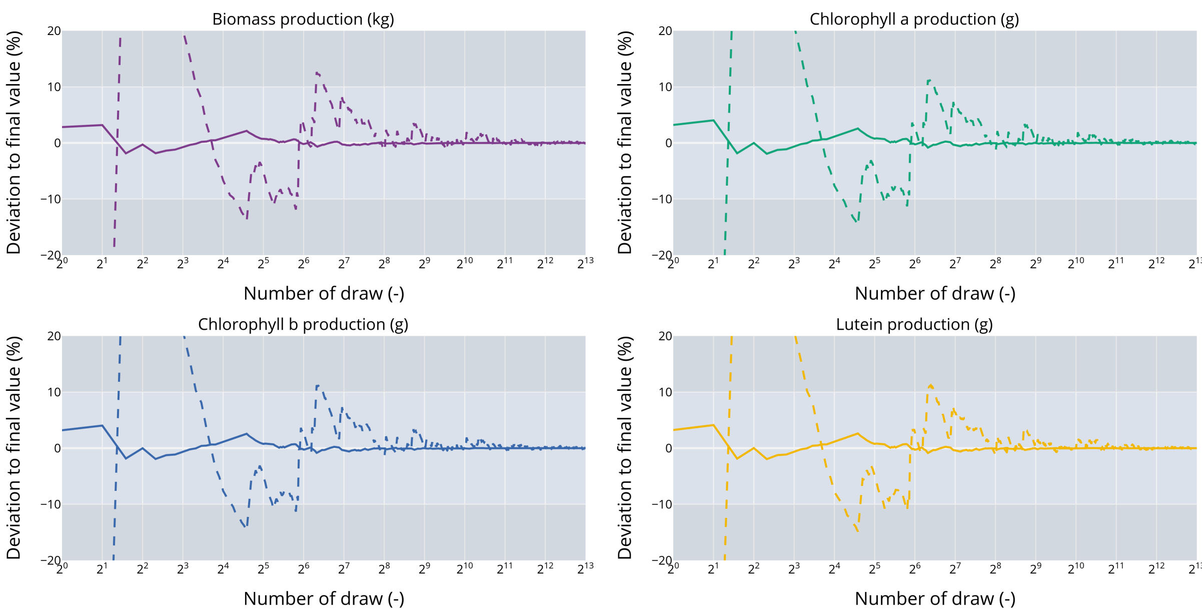

Fig. 1. Performance distribution arithmetic mean and standard deviation as function of the number of draw in the Sobol's sequence. Variation with respect to the values obtained with the highest number of draws

Nomenclature

Latin symbols	Property	Unit
A	First parameter of Defraeye's correlation	-
B	Second parameter of Defraeye's correlation	$W/m^2/K$
CC	Cloud Cover factor	-
Cp	Specific heat	J/kg/K
E	Elevation above the ground	m
e	Thickness	m
F	View factor	-
f	Areation	VVM (Vessel Volume per Minute)
H	Height	m
h	Convective heat transfer coefficient	$W/m^2/K$
k	Thermal conductivity	W/m/K
L	Characteristic length	m
n_X	Number of X	-
P	Power	W
Pr	Prandtl number	-
Re	Reynolds number	-
R	Reflectivity	-
Ra	Rayleigh number	-
r	Surface roughness	m
T	Temperature	°C in the text / K in formulas
t	Time	s
U	Velocity	m/s
UHII	Urban Heat Island Intensity	K
w	Width	m
Y	Relative humidity	%

Greek symbols	Property	Unit
α	Green light transmitted fraction	-
ϵ	Emissivity	-
η	Efficiency	-
θ	Angle	rad
ρ	Density	kg/m^3
σ	Boltzmann's constant	$W/m^2/K^4$
τ	Transmission	-
Φ	Heat flux	W/m^2

Subscript	Description
Abs	Absorbed by the culture
Air	Air, indoor or outdoor
Building	Building hosting the facade
Conv	Convective-conductive
Emi	Emitted
Forced	Forced convection
Free	Free convection
Gas	Sparged gas
Glaz	Glazing
i	Incidence
In	Indoor
Interface	Interface
IR	Infrared
mc	Microalgae culture
Net	Net exchange
Out	Outdoor
pmma	PolyMethyl MethAcrylate
ps	Photosynthesis
r	Refraction
Rad	Radiative
Ref	Reference
Rur	Rural
Sky	Sky
Station	Meteorological station
Sun	Sun
Sur	Surrounding
Tot	Total
Urb	Urban
Vis	Visible
Water	Water
Wind	Wind

References

1. Recommended Practice for the Calculation of Daylight Availability. *Journal of the Illuminating Engineering Society*, 13(4):381–392, July 1984. ISSN null. . Publisher: Taylor & Francis _eprint: https://doi.org/10.1080/00994480.1984.10748791.
2. Xin-Guang Zhu, Stephen P Long, and Donald R Ort. What is the maximum efficiency with which photosynthesis can convert solar energy into biomass? *Current Opinion in Biotechnology*, 19(2):153–159, April 2008. ISSN 0958-1669. .
3. Luca Evangelisti, Claudia Guattari, and Francesco Asdrubali. On the sky temperature models and their influence on buildings energy performance: A critical review. *Energy and Buildings*, 183:607–625, January 2019. ISSN 0378-7788. .
4. Joe A. Clarke. *Energy Simulation in Building Design.* Routledge, 2001. ISBN 978-0-7506-5082-3. Google-Books-ID: WH0VCiF8jkoC.
5. Tomáš Ficker. Letter to the editor: Revision of the universal sky temperature model. *Indoor and Built Environment*, 31(9):2366–2369, November 2022. ISSN 1420-326X. . Publisher: SAGE Publications Ltd STM.
6. Se Woong Kim and Robert D. Brown. Urban heat island (UHI) intensity and magnitude estimations: A systematic literature review. *Science of The Total Environment*, 779:146389, July 2021. ISSN 0048-9697. .
7. Peter Hoffmann, Oliver Krueger, and K. Heinke Schlünzen. A statistical model for the urban heat island and its application to a climate change scenario. *International Journal of Climatology*, 32(8):1238–1248, 2012. ISSN 1097-0088. . _eprint: https://onlinelibrary.wiley.com/doi/pdf/10.1002/joc.2348.
8. Jiameng Lai, Wenfeng Zhan, Fan Huang, James Voogt, Benjamin Bechtel, Michael Allen, Shushi Peng, Falu Hong, Yongxue Liu, and Peijun Du. Identification of typical diurnal patterns for clear-sky climatology of surface urban heat islands. *Remote Sensing of Environment*, 217:203–220, November 2018. ISSN 0034-4257. .
9. Kevin Gallo, Robert Hale, Dan Tarpley, and Yunyue Yu. Evaluation of the Relationship between Air and Land Surface Temperature under Clear- and Cloudy-Sky Conditions. *Journal of Applied Meteorology and Climatology*, 50(3):767–775, March 2011. ISSN 1558-8424, 1558-8432. . Publisher: American Meteorological Society Section: Journal of Applied Meteorology and Climatology.
10. John R. Howell, M. Pinar Mengüc, Kyle Daun, and Robert Siegel. *Thermal Radiation Heat Transfer.* CRC Press, Boca Raton, 7th edition edition, December 2020. ISBN 978-0-367-34707-9.
11. Sheng Zhang, Dun Niu, and Zhang Lin. Mean radiant temperature calculated based on radiant heat dissipation of human body addressing effect of emissivity of inner surfaces of envelope. *Solar Energy*, 246:14–22, November 2022. ISSN 0038-092X. .
12. A. J. N. Khalifa and R. H. Marshall. Validation of heat transfer coefficients on interior building surfaces using a real-sized indoor test cell. *International Journal of Heat and Mass Transfer*, 33(10):2219–2236, October 1990. ISSN 0017-9310. .
13. Theodore L. Bergman, Adrienne S. Lavine, Frank P. Incropera, and David P. DeWitt. *Fundamentals of Heat and Mass Transfer, 8th Edition.* Wiley, 8th edition edition, May 2017.
14. Thijs Defraeye and Jan Carmeliet. A methodology to assess the influence of local wind conditions and building orientation on the convective heat transfer at building surfaces. *Environmental Modelling & Software*, 25(12):1813–1824, December 2010. ISSN 1364-8152. .